

Shaking table test and numerical analysis of a combined energy dissipation system with metallic yield dampers and oil dampers

Qiang Zhou[†]

*Institute of Civil Engineering and Architecture, Wuhan University of Technology,
Wuhan, 430070, P.R. China*

Xilin Lu[‡]

*State Key Laboratory for Disaster Reduction in Civil Engineering, Tongji University,
Shanghai, 200092, P.R. China*

(Received July 2, 2001, Accepted November 10, 2003)

Abstract. A shaking table test on a three-story one-bay steel frame model with metallic yield dampers and their parallel connection with oil dampers is carried out to study the dynamic characteristics and seismic performance of the energy dissipation system. It is found from the test that the combined energy dissipation system has favorable reducing vibration effects on structural displacement, and the structural peak acceleration can not evidently be reduced under small intensity seismic excitations, but in most cases the vibration reduction effect is very good under large intensity seismic excitations. Test results also show that stiffness of the energy dissipation devices should match their damping. Dynamic analysis method and mechanics models of these two dampers are proposed. In the analysis method, the force-displacement relationship of the metallic yield damper is represented by an elastic perfectly plastic model, and the behavior of the oil damper is simulated by a velocity and displacement relative model in which the contributions of the oil damper to the damping force and stiffness of the system are considered. Validity of the analytical model and the method is verified through comparison between the results of the shaking table test and numerical analysis.

Key words: metallic yield damper; oil damper; combined energy dissipation system; analysis model; shaking table test.

1. Introduction

Energy dissipation system is one of the most effective approaches to reduce seismic response of a structure, and has received more and more attention during the last 20 years. Generally speaking, there are four kinds of energy dissipation systems that include metallic yield damper, friction damper, viscoelastic damper and viscous fluid damper. Hanson *et al.* has reviewed the state-of-the-

[†] Lecturer

[‡] Professor and Director

art and state-of-the-practice in seismic energy dissipation (1993). Housner *et al.* gave a more wide review on structural control (1997). Kobori described the mission and perspective towards future structural control research (1998). Soong and Spencer gave a recent development review on semi-active and hybrid control of structure (2000).

During the last 20 years, single energy dissipation system has been studied more extensively and seismic regulations (codes) for passive structural control system have been developed in the US (Kircher 1998). Makris, Constantinou and Taylor have carried out a series of testing and modeling of viscous fluid dampers and their application in seismic energy dissipation and seismic isolation (Makris and Constantinou 1990, Constantinou *et al.* 1993, Taylor 1996). For the research and application of friction dampers, Pall developed a series of friction dampers that can be installed with braces in frame structures (1982). Aiken and Kelly carried out earthquakes simulator testing and analytical studies of Sumitomo dampers for multistory structure (1990). Metallic yield dampers are the earlier used dampers in seismic engineering practice. Kelly, Skinner and Heine studied the mechanism of energy absorption with metal plastic deformation for use in earthquake resistant structure (1972). Xia and Hanson studied the influence of added damping and stiffness (ADAS) device on structure seismic response and established a design methodology (1992). Whittaker *et al.* did some seismic testing of steel plate energy dissipation devices (1991). Tsai *et al.* developed a series of steel triangular plate energy absorbers for seismic resistant structures (1993). Although the various single energy dissipation systems has been studied extensively, it still has some limitation in engineering practice. Therefore, a combination mechanism, which incorporates a friction damping device or a metallic yield damping device for control of structural damage due to severe earthquake motion and a viscoelastic damping device for control of low energy excitation, such as wind forces or mild ground movements, has been developed in recent years (Pong *et al.* 1994, Tsiatas and Daly 1994, Sano *et al.* 1998). This paper describes the author's development of a combined energy dissipation system that is composed of metallic yield dampers and their parallel connection with oil dampers in frame braces. Firstly, the concept and mechanism of the combined system is introduced. Secondly, a series of shaking table tests on a frame model under different seismic inputs are carried out to evaluate the performance of the combined system. Then an analysis method for the system is proposed and verified by the test results.

2. The combined energy dissipation system

The combined energy dissipation system proposed in the paper consists of the following parts: metallic yield damper, oil damper and conventional steel brace. Their installation in a frame is shown in Fig. 1. The steel brace is connected by the metallic yield damper to the upper beam, and the oil damper is connected to the brace and the upper beam. By this connection the metallic yield damper and the oil damper has the parallel effect in resisting the lateral forces, and resistant forces of the metallic yield damper and the oil damper are transferred to the upper beam and then to the columns. This connection can also avoid the stress concentration in columns when oil dampers are connected directly with columns.

The working mechanism of the combined energy dissipation system is as follow. Under wind load or lower earthquake intensity, the metallic yield damper behaves elastically and the oil damper provides smaller damping force and some stiffness. Under stronger earthquake the metallic yield damper develops elastoplastic deformation and the stiffness to the structure is decreased, and the oil

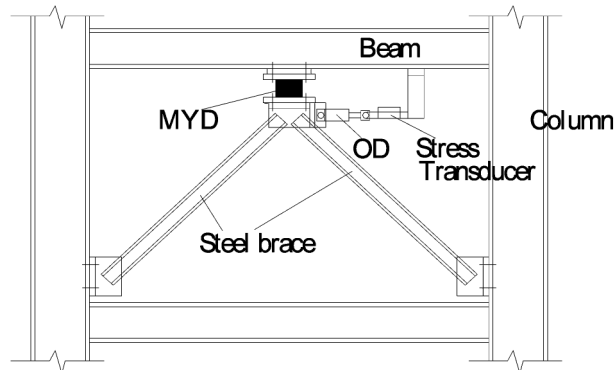


Fig. 1 The installation of the combined energy dissipation system in a frame

damper provides larger damping force and also some stiffness. As a result, the seismic force to the whole structure is reduced and its response decreased. In engineering application the combined energy dissipation system can be installed in a braced frame. It must be noted that, whether the combined energy dissipation system is effective or not, the key point is that equivalent damping coefficient and stiffness of the two dampers should be matched.

3. Performance tests of the combined energy dissipation system

3.1 Outline of the test frame

A three-story steel frame is used as the test model. Fig. 2 shows the size of the model and the

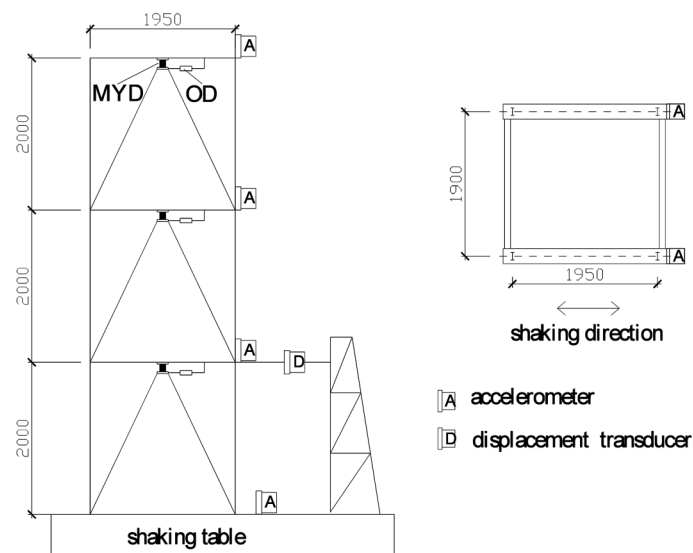


Fig. 2 The size of the test frame and transducer arrangement

transducer arrangements on the model, in which A denotes accelerometer, D denotes displacement transducer, MYD denotes metallic yield damper and OD denotes oil damper. The section area of the columns is 14.33 cm^2 and the moment of inertia in vibration direction is 32.8 cm^4 . The section area of the beam is 15.69 cm^2 and the moment of inertia in vibration direction is 391.0 cm^4 . The section area of the brace is 6.9 cm^2 . In order to make the fundamental frequency of the testing frame equal to 1.0 Hz that is close to the frequency of a typical high-rise building, additional mass was applied to each floor by bolting it to the floor beam. The total masses from the first floor to the top floor including frame self-weight during testing are 1478.25 kg , 1478.25 kg and 1832.25 kg , respectively.

3.2 Dampers and their parameters

The metallic yield dampers used in the test are shown in Fig. 3, and welding manner is used to connect each part. The dimension of the damper can be designed according to the properties of main frame and energy dissipation system. The modulus of elasticity and yield stress of steel are $2.06 \times 10^{11} \text{ N/m}^2$ and $2.15 \times 10^8 \text{ N/m}^2$ respectively. The force-displacement relationship of the metallic yield damper is represented by an elastic perfectly plastic model, as shown in Fig. 4, in which the initial stiffness K_i and yield load F_y are

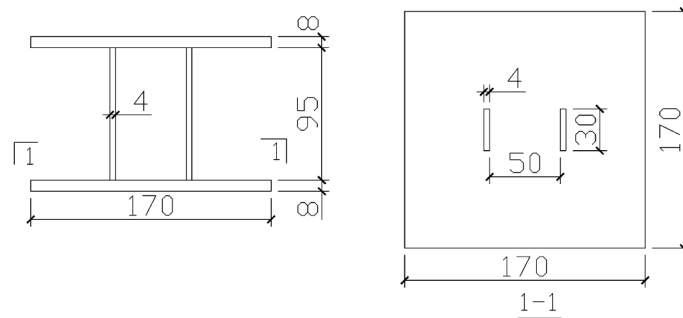


Fig. 3 Outline of the metallic yield damper (unit: mm)

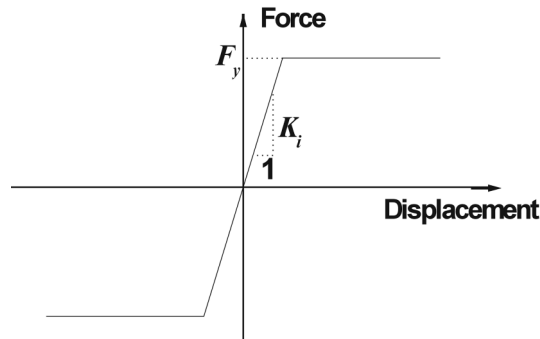


Fig. 4 Relationship between force and displacement of the metallic yield damper

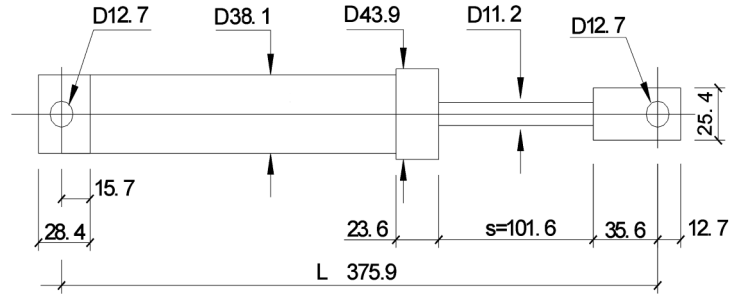


Fig. 5 Outline of the oil damper (unit: in)

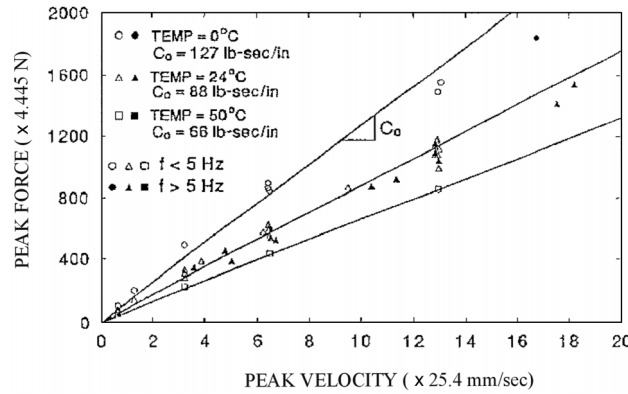


Fig. 6 Relationship between maximum damping force and maximum velocity under different temperature

$$K_i = \frac{24EI}{l^3} = \frac{24 \times 2.06 \times 10^{11} \times (0.03 \times 0.004^3 / 12)}{0.095^3} = 9.226 \times 10^5 \text{ N/m} \quad (1)$$

$$F_y = \frac{bh^2}{l} \sigma_y = \frac{0.03 \times 0.004^2}{0.095} \times 2.15 \times 10^8 = 1086.3 \text{ N} \quad (2)$$

The oil damper used in the test is D-series linear damper whose maximum damping force is 8.88 kN. The dimension of the damper is shown in Fig. 5, and the relationship of maximum damping force and maximum velocity under different temperature is shown in Fig. 6.

The combination and installation of the metallic yield damper and the oil damper in a frame is shown in Fig. 1 (see section 2). There are six combined energy dissipation braces installed symmetrically in the test frame in order to avoid eccentric vibration during the testing.

3.3 Input to the model and instrumentation

In order to evaluate the performance of the combined energy dissipation system under various seismic excitation, five earthquake acceleration records were selected as the input data during the

shaking table testing, which are El Centro (1940, NS), Taft (1952, NS), Northridge (1994), Kobe (1995) and Shanghai design code specified artificial earthquake accelerogram (SHW2, 1996). All the earthquake acceleration records are inputted in only one direction of the test model, and the time interval is 0.01 second. The peak ground acceleration (PGA) was increased gradually from 100 gal to 400 gal. Two accelerometers were installed at every floor. Since it is very difficult to measure displacement at roof level during larger deformation, only one displacement transducer was connected to the first floor. There was one tension and compression transducer connected to each oil damper to measure the damping force during testing. All the test data were collected by computer-controlled data acquisition system and transferred to a PC for further analysis.

3.4 Dynamic characteristics of the test frame

White noise scan test was done to obtain the dynamic characteristics of the model. The peak value of the white noise input was selected to 50 gal in order to keep the model in linear elastic deformation. To make comparison three conditions of the model were tested during this stage: unbraced frame (UF), frame braced with the metallic yield damper and steel brace (MYD), frame braced with combination of the metallic yield damper, oil damper and steel brace (MYD+OD)

The fundamental frequency and damping ratio are shown in Table 1. The following points can be drawn from Table 1. (1) The frequency and damping ratio of MYD frame are larger than those of unbraced frame, which means the metallic yield damper can provide apparent stiffness and damping to the system. (2) The frequency and damping ratio of MYD+OD frame are larger than those of MYD frame, which shows the oil damper can provide not only damping but also some stiffness to the system. Therefore, in analytical model this behavior of the oil damper should be simulated properly.

Table 1 Frequency and damping ratio of the test frame

	Test frame with dampers		Test frame without dampers
	MYD only	MYD+OD	
Fundamental frequency (Hz)	2.539	3.027	1.074
Damping ratio	0.046	0.124	0.010

3.5 Dynamic response of the test frame

The uniform index, which is used to evaluate vibration-reducing effect, is defined as

$$\text{vibration reduction index} = \frac{R_n - R_f}{R_n} \quad (3)$$

where R_f and R_n are the response of the structure with and without dampers respectively.

The maximum acceleration responses at roof level of the test frame are shown in Table 2 for the entire test. It can be found that: (1) MYD frame has smaller response of acceleration compared with the unbraced frame except under El Centro record (100 gal) input, and vibration reduction index is in the range of 24%-64%. (2) MYD+OD frame under various smaller seismic inputs (100 gal) has

Table 2 Maximum acceleration at roof level of the test frame (gal)

Seismic input	Peak value of the input (gal)	Test frame with dampers		Test frame without dampers
		MYD only	MYD+OD	
El-Centro	100	135	201	130
	200	153	269	249
	300		281	350
	400	205	295	445
Kobe	100	113	149	148
	200	160	225	261
	300		307	
	400	359	364	
Northridge	100	111	145	146
	200	158	244	316
	300		271	
	400		323	
Taft	100	122	188	173
	200	159	200	273
	300		244	
	400	189	252	
SHW2	100	122	193	264
	200	211	283	399
	300		344	
	400		436	

hardly any vibration reduction effect. However, under larger seismic inputs, the combined energy dissipation system can effectively reduce acceleration response. (3) The vibration reduction effect under large seismic inputs (300 gal and 400 gal) is better than that of the response under smaller seismic inputs (100 gal and 200 gal), which means that under larger seismic inputs, the stiffness contribution to the frame provided by dampers become small, and the damping contribution to the frame become larger. (4) MYD+OD frame has larger response of acceleration compared with MYD frame. The reason is that the oil damper can provide not only damping but also some stiffness to the system, so the response of the system can not be certainly reduced after oil damper is connected in parallel. Therefore, there exists proper match between equivalent damping coefficient and stiffness of the two dampers, which should be prudently selected. (5) Under different seismic inputs the vibration reduction effect is different. Therefore the selection of the stiffness and damping of the energy dissipation system is not only related to structural behavior of the frame but also to the characteristics of the acceleration time history of the construction site where the frame structure will be built.

Through twice integral of the relative acceleration time history, one can obtain the displacement time history. There is a good agreement between measured value and calculated value of the displacement of the first floor under various seismic excitations, as shown in Fig. 7.

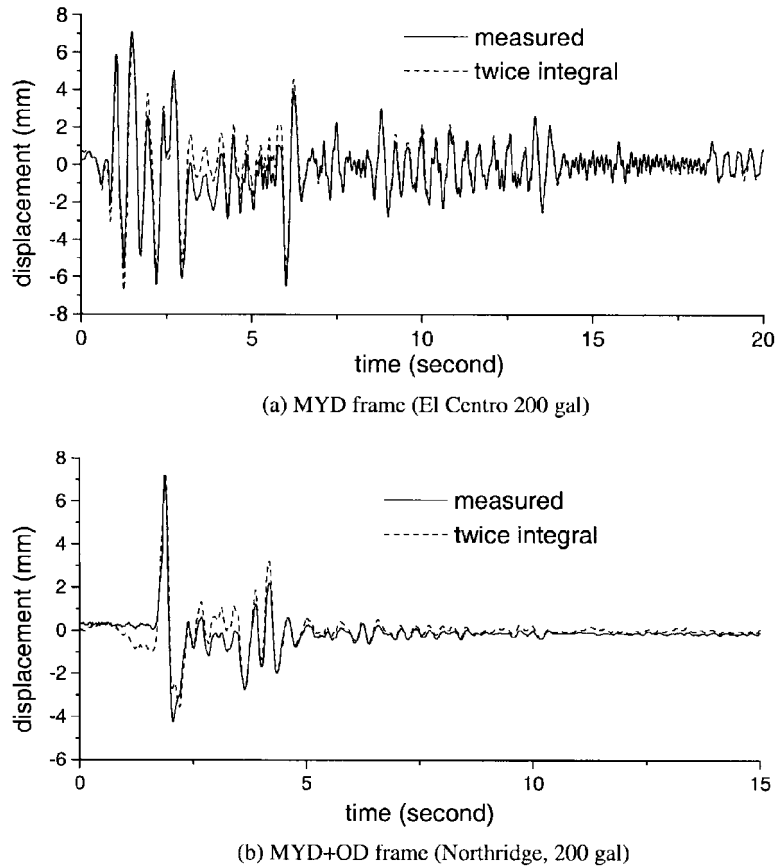


Fig. 7 Displacement of the first floor under various seismic record input

The maximum displacement responses at roof level of the test frame are listed in Table 3. One can find that generally the displacement responses of the frame with dampers are smaller than those of the unbraced frame in all seismic inputs with different intensities, which means that the dampers have provided stiffness and damping to the frame structure. The vibration reduction index for the displacement of MYD frame is in the range of 61%-86%, and that of MYD+OD frame is in the range of 59%-85%, which are better than the index for the acceleration. It should be noted that the displacement responses of MYD+OD frame are not evidently decreased compared with those of MYD frame.

The maximum shear force at the first floor of the test frame is listed in Table 4. It can be found that: (1) The shear force of MYD frame is smaller than that of the unbraced frame, in most cases, the index is in the range of 11%-39%. (2) The shear force is not evidently decreased after installing metallic yield damper and oil damper in the unbraced frame. In some cases, the shear force is increased. (3) In most cases, the shear force of MYD+OD frame is 31 to 47 percent larger than that of MYD frame. The reason is explained as follows. The equivalent stiffness and damping coefficient of the first floor of the main frame are K_{ef} and C_{ef} respectively, and those of the damper are K_{ed} and C_{ed} respectively. The displacement and velocity of the first floor of the frame with and

Table 3 Maximum displacement at roof level of the test frame (mm)

Seismic input	Peak value of the input (gal)	Test frame with dampers		Test frame without dampers
		MYD only	MYD+OD	
El-Centro	100	7.708	8.840	30.138
	200	12.923	13.844	58.538
	300		16.304	86.209
	400	24.446	22.138	110.00
Kobe	100	9.628	9.059	29.776
	200	17.311	17.494	52.194
	300		23.941	
	400	42.318	31.391	
Northridge	100	5.766	5.944	35.034
	200	16.447	12.659	75.553
	300		17.962	
	400		35.836	
Taft	100	8.136	8.540	20.784
	200	11.487	11.572	37.321
	300		16.906	
	400	28.575	19.777	
SHW2	100	9.363	9.582	64.673
	200	24.659	23.129	112.35
	300		32.044	
	400		42.034	

without dampers are x_d , \dot{x}_d , x_f and \dot{x}_f respectively. Then the maximum shear force of the first floor of the frame with and without dampers is S_d and S_f respectively, which can be represented as

$$S_d = \max\{(K_{ef} + K_{ed}) \times x_d + (C_{ef} + C_{ed}) \times \dot{x}_d\} \quad (4)$$

$$S_f = \max(K_{ef} \times x_f + C_{ef} \times \dot{x}_f) \quad (5)$$

Although x_d and \dot{x}_d are smaller than x_f and \dot{x}_f , S_d contains force provided by the damper ($K_{ed} \times x_d + C_{ed} \times \dot{x}_d$), so in some cases it is possible that S_d is greater than S_f . Therefore, there exists proper match between equivalent damping coefficient and stiffness of the two dampers, which should be carefully selected.

The responses of time history of the test frame with the energy dissipation system are also much smaller than those of unbraced frame. Due to the length limitation of the paper, only some of the time histories are presented herein. Fig. 8 and Fig. 9 show the displacement and acceleration time history at roof level of the test frame under El Centro (200 gal) excitation respectively. From Fig. 8 one can see that the energy dissipation system can rather effectively reduce displacement response.

From Fig. 9 one can find that, even the combined energy dissipation system can not reduce the maximum response of acceleration, it makes the response in most of the duration time is reduced apparently.

Table 4 Maximum shear force at the first floor of the test frame (kN)

Seismic input	Peak value of the input (gal)	Test frame with dampers		Test frame without dampers
		MYD only	MYD+OD	
El-Centro	100	3.878	5.684	3.847
	200	5.518	7.712	7.270
	300		8.388	9.063
	400	7.557	9.487	11.436
Kobe	100	4.445	6.161	3.859
	200	5.575	9.431	7.118
	300		11.854	
	400	10.497	13.832	
Northridge	100	3.072	4.034	3.681
	200	5.478	6.662	8.068
	300		8.446	
	400		12.906	
Taft	100	3.742	5.838	4.210
	200	4.513	6.304	7.119
	300		8.569	
	400	7.895	9.232	
SHW2	100	4.396	6.200	7.166
	200	7.281	11.876	11.814
	300		13.312	
	400		15.787	

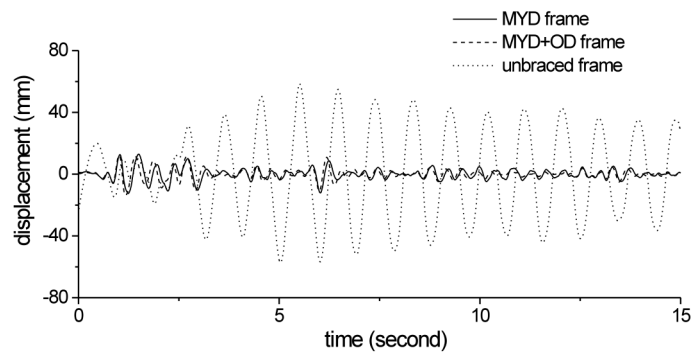


Fig. 8 Displacement time history at roof level of the test frame under El Centro (200 gal) input

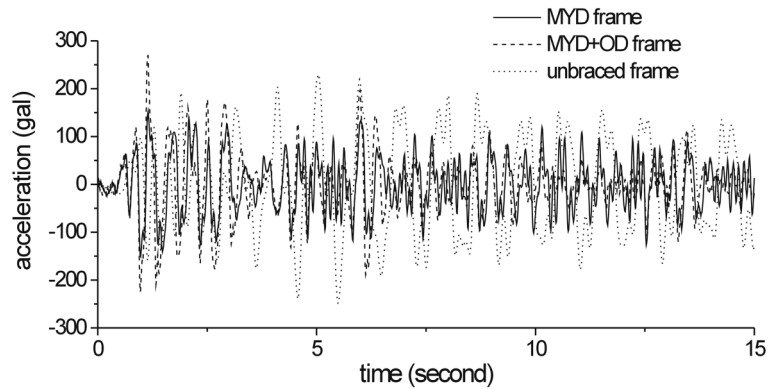


Fig. 9 Acceleration time history at roof level of the test frame under El Centro (200 gal) input

4. Analysis method and its verification

4.1 Analytical model for the test frame

Since the test frame is symmetric and seismic input is only in one direction, the plane frame model can be used to simulate the test frame, and the analytical model is shown in Fig. 10 in which only elastic deformation is considered for the steel members such as beams and columns. Because the stiffness of braces is far larger than that of columns and dampers, the deformation of the brace is ignored and the deformation of damper is approximately equal to inter-storey drift of the floor.

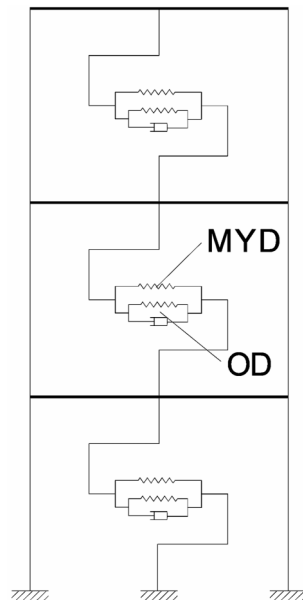


Fig. 10 Analytical model of the test frame with the energy dissipation system

4.2 Simulation of dampers in the analytical model

The force-displacement relationship of the metallic yield damper is represented by an elastic perfectly plastic model, as shown in Fig. 4, in which two main parameters K_i and F_y are presented by Eqs. (1) and (2) respectively.

According to Table 1, the oil damper not only provides damping force to the test frame but also some stiffness to the system. Therefore the following equation is used to simulate the viscous damping force of the oil damper.

$$F(x, \dot{x}) = c_d \dot{x} + k_d x \quad (6)$$

In which, x and \dot{x} are the inter-storey drift and velocity of the floor where the oil damper is installed, and c_d and k_d are the parameters related to the oil damper. In this study, c_d is taken as 15.45 kN sec/m and $k_d = 100.0$ kN/m.

The dynamic equation of the whole system can be expressed by the following equation

$$[M]\{\ddot{x}\} + [C]\{\dot{x}\} + \{F\} = -[m]\{I\}\ddot{x}_g \quad (7)$$

Where $[M]$ and $[C]$ are the mass and damping matrix respectively, $\{F\}$ is the restoring force vector that includes the restoring force of the frame and the energy dissipation devices, $\{x\}$ is the displacement vector, $\{I\}$ is a unit vector and \ddot{x}_g is the input acceleration. The above Eq. (7) can be solved by Newmark integration and Newton-Raphson iterative procedure (Bathe 1982), with the following numerical value for the unbraced frame model.

$$m = \begin{bmatrix} 739.125 & 0 & 0 \\ 0 & 739.125 & 0 \\ 0 & 0 & 916.125 \end{bmatrix} \quad k = \begin{bmatrix} 407546.2 & -207766.9 & 7912.4 \\ -207766.9 & 399352.9 & -199223.2 \\ 7912.4 & -199223.2 & 191262.7 \end{bmatrix} \quad (8)$$

$$c = \begin{bmatrix} 98.0 & 0 & 0 \\ 0 & 98.0 & 0 \\ 0 & 0 & 121.5 \end{bmatrix}$$

For the energy dissipation system, the stiffness and damping force should be added to the above Eq. (7), and then the vibration frequency and dynamic response of the system can be obtained. Table 5 shows the fundamental frequency calculated by the above procedure and comparison with the test results. It can be seen that there is a sound agreement between test and analysis. Due to the

Table 5 Comparison of the tested frequency and calculated one of the test frame (Hz)

	Tested frame with dampers		Tested frame without dampers
	MYD only	MYD+OD	
Calculated value	2.583	3.019	1.057
Tested value	2.539	3.027	1.074
Error	1.7%	0.3%	1.6%

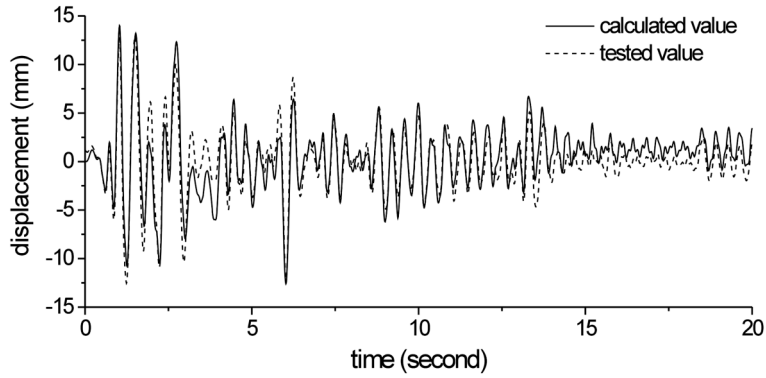


Fig. 11 Displacement time history at roof level of the test frame with metallic yield dampers under El Centro (200 gal) input

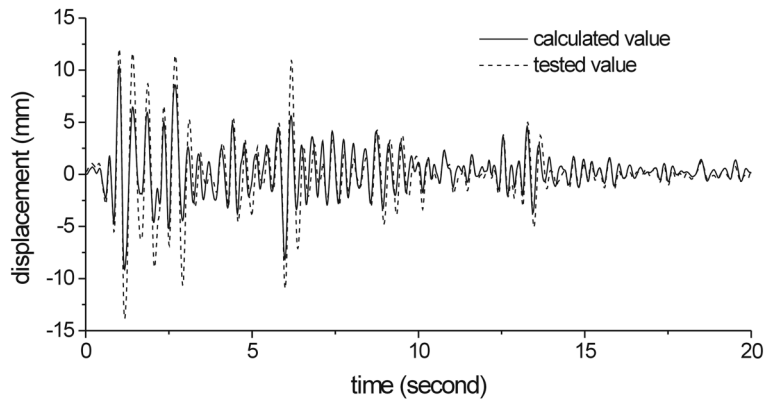


Fig. 12 Displacement time history at roof level of the test frame with combined energy dissipation system under El Centro (200 gal) input

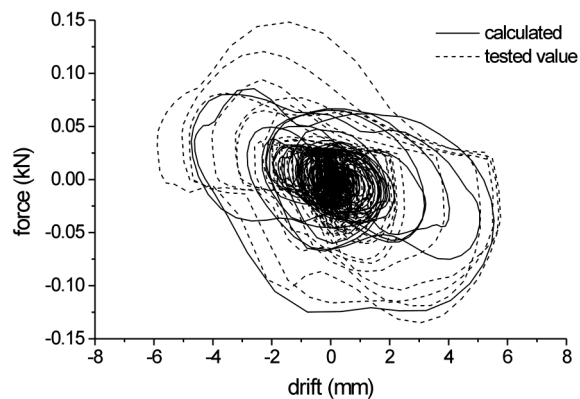


Fig. 13 Relationship between the drift of the first floor and the damping force of the oil damper under El Centro (200 gal) input

length limitation of the paper, only the calculated and tested displacement of roof level and force-deformation of the oil damper of the first floor time histories under El Centro (200 gal) input are presented herein, as shown in Fig. 11 to 13. One can find that there is a good agreement between the analysis and test results, which demonstrates that the analysis model and method proposed are valid and reasonable for the dynamic analysis of the energy dissipation system.

5. Conclusions

Based on the above-mentioned test and analysis of the two energy dissipation systems, the following conclusions can be drawn:

1. Both energy dissipation systems in this study have good performance in reducing the seismic response of structure in terms of displacement. The vibration reduction effect becomes better as the seismic input is increased. But the base shear of the energy dissipation system is not always smaller than that of unbraced frame.

2. The oil damper can provide not only damping force to the combined energy dissipation system, but also some stiffness to the system. Therefore the response of the system can not be certainly reduced after oil damper is connected in parallel. The various vibration reduction index of the system, including displacement and shear force of the first floor and acceleration of roof level, has not been improved after installing oil dampers in the frame with metallic yield dampers in the test. In some cases, the seismic response of the combined energy dissipation system may be increased. Therefore, there exists proper match between equivalent damping coefficient and stiffness of the two dampers, which should be carefully selected.

3. The proposed method for simulating the behavior of metallic yield damper and oil damper is verified by shaking table test results, and there is a good agreement between simulation results and test ones. Therefore this method can be used in the analysis of energy dissipation system for engineering practice.

Acknowledgements

The financial support of National Nature Science Foundation of China through grant 50025821 is gratefully acknowledged.

References

- Aiken, J.D. and Kelly, J.M. (1990), "Earthquake simulator testing and analytical studies of two energy-absorbing systems for multistory structure", *Report No. UCB/ERC-90/03*, Earthquake Engineering Research Center, Univ. of California, Berkeley, CA
- Bathe, K.J. (1982), *Finite Element Procedures in Engineering Analysis*, Prentice-Hall, Inc.
- Constantinou, M.C. *et al.* (1993), "Fluid viscous dampers in application of seismic energy dissipation and seismic isolation", *Proc. of ACT-17-1 on Seismic Isolation, Energy Dissipation and Active Control*, **2**, 581-592.
- Hanson, R.D. *et al.* (1993), "State-of-the-art and state-of-the-practice in seismic energy dissipation", *Proc. of ACT-17-1 on Seismic Isolation, Energy Dissipation and Active Control*, **2**, 449-471.

- Housner, G.W. *et al.* (1997), "Structural control: past, present and future", *J. Engrg. Mech.*, ASCE, **123**, 897-971.
- Kelly, J.M., Skinner, R.I. and Heine, A.J. (1972), "Mechanisms of energy absorption in special devices for use in earthquake-resistant structure", *Bull. N. Z. Nat. Soc. for Earthquake Engrg.*, **5**, 63-88.
- Kircher, C. (1998), "Seismic regulations for passive structural control systems-overview of United States codes", *Proc. 2nd World Conf. on Struct. Control*, **3**, 2441-2450.
- Kobori, T. (1998), "Mission and perspective towards future structural control research", *Proc. 2nd World Conf. on Struct. Control*, **1**, 23-34.
- Makris, N. and Constantinou, M.C. (1990), "Viscous dampers: testing, modeling and application in vibration and seismic isolation", *NCEER Rep. 90-0028*, State Univ. of New York at Buffalo, Buffalo, N.Y.
- Pall, A.S. and Marsh, C. (1982), "Response of friction damped braced frames", *J. Struct. Div.*, ASCE, **108**, 1313-1323.
- Pong, W.S., Tsai, C.S. and Lee, G.C. (1994), "Seismic study of viscoelastic dampers and TPEA devices for high-rise buildings", *Proc. 1st World Conf. Struct. Control*, **1**, WP3 23-31.
- Sano, T., Takahashi, Y. and Suzuki, T. (1998), "Development of hybrid damping system for seismic vibration control: performance test and vibration control effect study on Y-O damper", *Proc. 2nd World Conf. on Struct. Control*, **1**, 276-286.
- Soong, T.T. and Spencer, B.F. (2000), "Seismic-active and hybrid control of structures", *Proc. 12th World Conf. Earthquake Engrg.*, Paper No. 2834.
- Taylor, D.P. (1996), "Fluid dampers for applications on seismic energy dissipation and seismic isolation", *Proc. 11th World Conf. Earthquake Engrg.*, Paper No. 798.
- Tsai, K.C. *et al.* (1993), "Design of steel triangular plate energy absorbers for seismic resistant construction", *Earthquake Spectra*, **9**, 505-528.
- Tsiatas, G. and Daly, K. (1994), "Controlling vibrations with combination viscous/friction mechanisms", *Proc. 1st World Conf. Struct. Control*, **1**, WP4 3-11.
- Whittaker, A.S. *et al.* (1991), "Seismic testing of steel plate energy dissipation devices", *Earthquake Spectra*, **7**, 563-604.
- Xia, C. and Hanson, R.D. (1992), "Influence of ADAS element parameters on building seismic response", *J. Struct. Engrg.*, ASCE, **118**, 1903-1918.